

Operation parameters of melt spinning of polypropylene hollow fiber membranes

Jae-Jin Kim ^{a,*}, Jeong Rim Hwang ^a, Un Young Kim ^a, Sung Soo Kim ^b

^a Membrane Laboratory, The Korea Institute of Science and Technology P.O. Box 131, Cheongryang, Seoul, South Korea

^b Department of Chemical Engineering, Kyung Hee University, Seoul, South Korea

Received 28 April 1994; revised 10 April 1995; accepted 11 May 1995

Abstract

Microporous hollow fiber membranes were prepared via melt spinning of a polypropylene/soybean oil mixture. Many operation parameters of melt spinning process were examined in terms of the structure variation by scanning electron microscopy and bubble point pressure measurement. The initial composition of the melt solution affected the porosity and the pore size of the membrane. Melt viscosity of the hollow fiber spun depended on the spinning temperature and affected the structure. Increased melt–draw ratio enhanced the formation of the micropores and fibril structure. Subsequent cold-stretching of the hollow fiber membrane produced tiny fibrils and micropores via stretching and cleavage. A combination of thermally-induced phase separation and cold-stretching produced an unusually highly porous membrane without significant changes of the inside and outside diameters of the hollow fiber membranes.

Keywords: Microporous membranes; Thermally-induced phase separation; Hollow fiber; Melt spinning; Polypropylene

1. Introduction

The thermally-induced phase separation (TIPS) process has been utilized for making microporous membranes [1–3]. Various polymers and diluents have been used for the TIPS process, and some of them have been commercialized [1–4]. Polypropylene (PP) is one of the most popular TIPS membrane materials because of its many advantages over other polymers [4]. The choice of diluent is important since it determines the interactions with the polymer and consequently the phase separation mechanism [4–7]. Soybean oil is an appropriate candidate for diluent, since it forms a homogeneous solution with PP at elevated temperatures and undergoes liquid–liquid phase

separation upon cooling. Moreover, soybean oil has little toxicity and is cheaper than previously reported diluents for PP.

For membrane preparation, the polymer/diluent melt is extruded and undergoes TIPS. In this study hollow fiber membranes were prepared from PP/soybean oil mixture via a melt spinning process. Melt spinning is a complex process, which can include factors other than TIPS upon cooling, such as stretching, diluent extraction, etc. There are many parameters in this process, which have great influences on the membrane structure formation, and some of them are difficult to be quantified experimentally. After several trials three parameters were chosen to be examined, initial composition of melt solution, spinning temperature, and melt–draw ratio.

* Corresponding author.

Table 1
Constituents of soybean oil

Constituents	Composition (%)
Linoleic acid	50.7
Oleic acid	28.9
Palmitic acid	9.8
Linolenic acid	6.5
Stearic acid	2.4
Arachidic acid	0.9
Palmitoleic acid	0.4
Lauric acid	0.2
Myristic acid	0.1
Others	0.1

The Celanese Corp. developed the technique of making microporous polymeric membranes by cold-stretching semi-crystalline polymeric films [8,9]. They produce various kinds of polypropylene Celgard[®] membranes. Gore applied a similar technique to make porous polytetrafluoroethylene films [10,11]. Mitsubishi Rayon Co. further developed the so-called melt spinning and cold-stretching (MSCS) process to make polypropylene and polyethylene hollow fiber membranes for various purposes [12,13]. In the MSCS process micropore formation results from lamellae spreading via cold-stretching [8,14]. The MSCS process has been applied to the dense and nonporous films or hollow fibers to make them porous. In this study the MSCS process was applied to the porous hollow fiber membrane preformed via TIPS based on the possibility that in the TIPS process microcrystalline lamellae also aligns despite the presence of diluent, and that the subsequent cold-stretching can still change the membrane structure.

2. Materials

PP was supplied by Daehan Yuhwa, Korea, and its weight average molecular weight was 400 000 and melt index was 2 g/10 min. Soybean oil was obtained from Cheil Food Chemicals, Korea, and its constituents are listed in Table 1. Trichlorotrifluoroethane (Freon 113) was purchased from Ulsan Chemicals, Korea, and ethyl alcohol, isopropyl alcohol, and *n*-hexane from Merck.

3. Generation of the phase diagram

Measured amounts of PP and diluent were mixed in a test tube and purged with nitrogen. The test tube was flame sealed and placed in an oven preset at 200°C for 24 h to make a homogeneous melt solution. The test tube was quenched in ambient water to recover the homogeneous sample. A Perkin–Elmer DSC 4 was used for the thermal analyses. The sample was placed in a DSC sample pan made for volatile compounds and was melted at 483 K and held there for 10 min. Then it was cooled at a rate of 10 K/min, and the exothermic peak temperature was taken as a dynamic crystallization temperature of the sample. A Mettler FP 82 hot stage and FP 80 central processor were used for cloud point measurement. The chopped sample was placed between a pair of microscope cover slips sealed with Teflon tape, placed on the hot stage apparatus preset at 483 K for 3 min, and cooled at a rate of 10 K/min, and onset of transmittance decrease was taken as the cloud point. Details of the cloud point measurement have been well described elsewhere [15,16].

As shown in Fig. 1, the phase diagram of PP/soybean oil system has a flat crystallization curve at concentrations less than the monotectic composition, which is a characteristic of liquid–liquid phase separation [16]. The dynamic monotectic point is located around 60 wt.% of PP and 378 K at a cooling rate of 10 K/min.

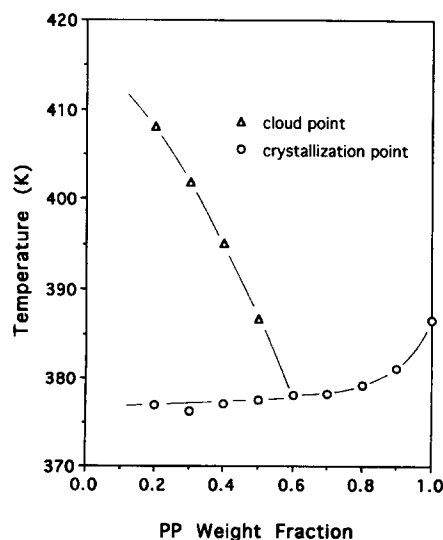


Fig. 1. Phase diagrams of the PP/soybean oil system determined at 10 K/min cooling.

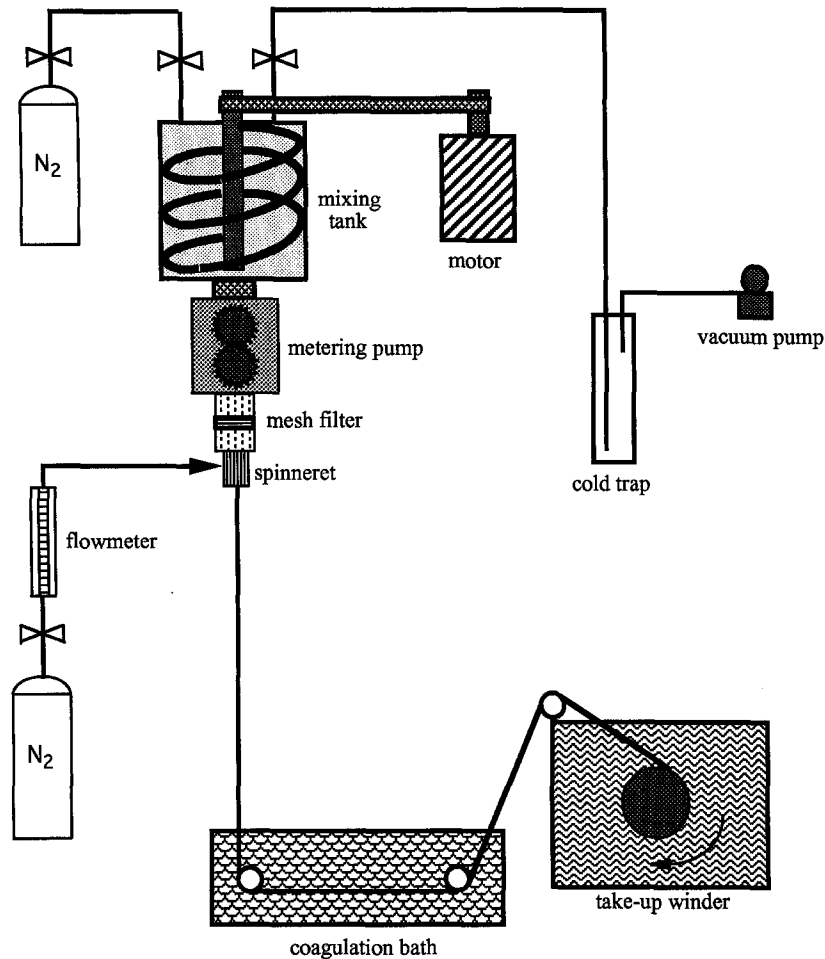


Fig. 2. A schematic diagram of the vessel extrusion apparatus.

4. Melt spinning of hollow fiber membranes

Hollow fibers were prepared via melt spinning. Difficulties in the premixing of PP and the liquid diluents and in feeding them through the hopper prevented use

of a conventional extruder. Therefore, a vessel extrusion apparatus was designed as shown in Fig. 2. Measured amounts of PP and diluent were placed in the vessel and heated to 493 K under a nitrogen purged atmosphere. The mixing blade was employed to

Table 2
Melt spinning conditions of the hollow fiber membranes under investigation

Figure numbers in text	Composition (wt.% of PP)	Spinning temperature (K)	Melt–draw ratio (%)
3 and 4		438	712
5	40	438	500
6 ^a , 7 and 8	40		712
6 ^b , 10 and 11	40	438	
12, 13 and 14	40	438	900

^a Spinning temperature plot.

^b Melt–draw ratio.

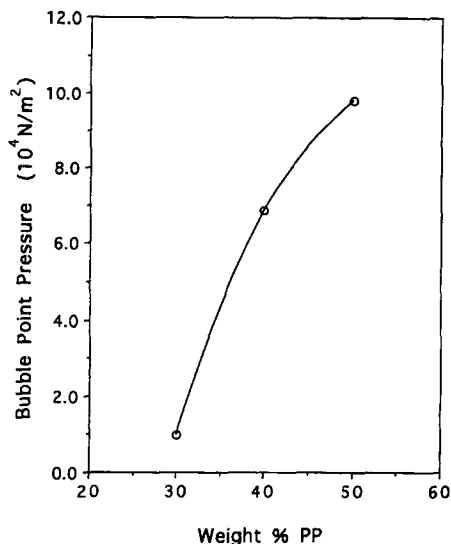


Fig. 3. Effect of PP composition of the melt solution on the bubble point pressure of the hollow fiber membranes.

enhance sample homogeneity, and the mixing time was 4 h. The mixing blade was designed in a spiral form to ensure complete mixing by scraping the wall of the vessel. Under nitrogen pressure a metered amount of the homogeneous melt was fed to a spinneret by a gear pump. A spinneret of the tube-in-orifice type was manufactured; i.d. 3 mm and o.d. 5 mm. Another stream of nitrogen was introduced into the spinneret to make a lumen at the center of the fiber. The spinning conditions of each hollow fiber membrane under investigation are listed in Table 2.

The hollow fiber melt was partly cooled in the air, and it entered the coagulation bath at $293 \pm 3 \text{ K}$, where it was completely solidified and stretched to reduce its final o.d. to $250 \mu\text{m}$. The Freon 113 in the coagulation bath was used as a diluent extractant as well as a coagulant, and diluent at the outer surface of the fiber was partly extracted while it passed through the coagulation bath. The hollow fiber was wound on a take-up winder at a specified melt–draw ratio. The remaining diluent was completely extracted in Freon 113 for 24 h. Finally, it was dried in a vacuum oven for the removal of the remaining solvent and diluent.

5. Structure analysis

The structure of each membrane was examined by using a scanning electron microscope (Hitachi S-510).

The bubble point pressure of each hollow fiber membrane was measured according to ASTM F 316-80 and E 128-61 specifications. The bath medium for bubble point pressure measurement was an ethyl alco-

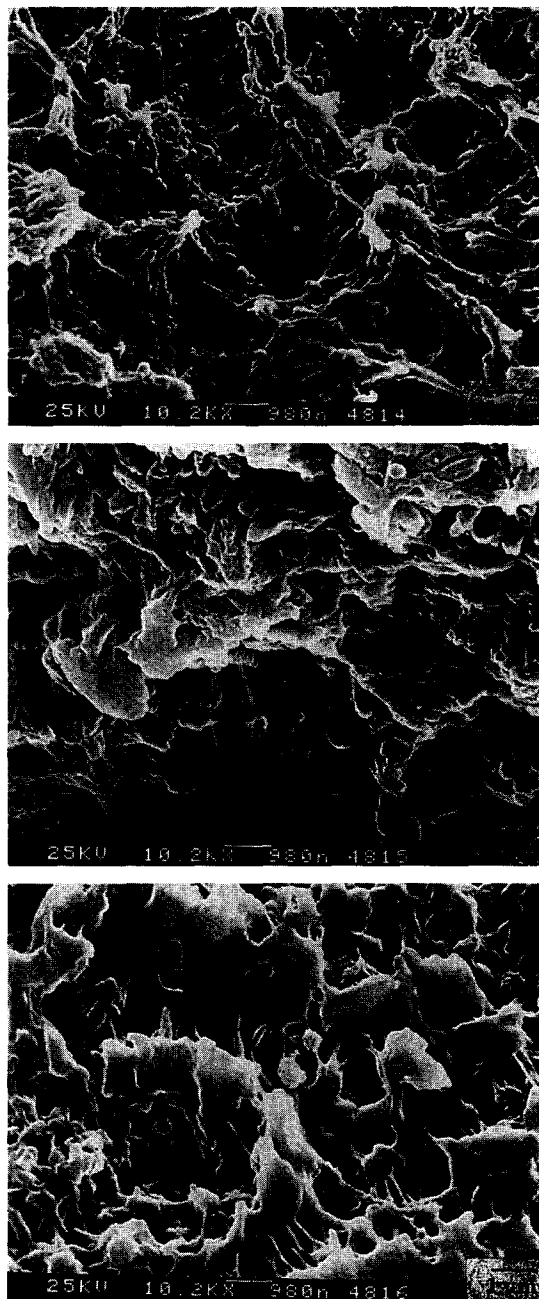


Fig. 4. Cross sectional images of the hollow fiber membranes made from different PP compositions (top, 30 wt.% of PP; middle, 40 wt.% of PP; bottom, 50 wt.% of PP).

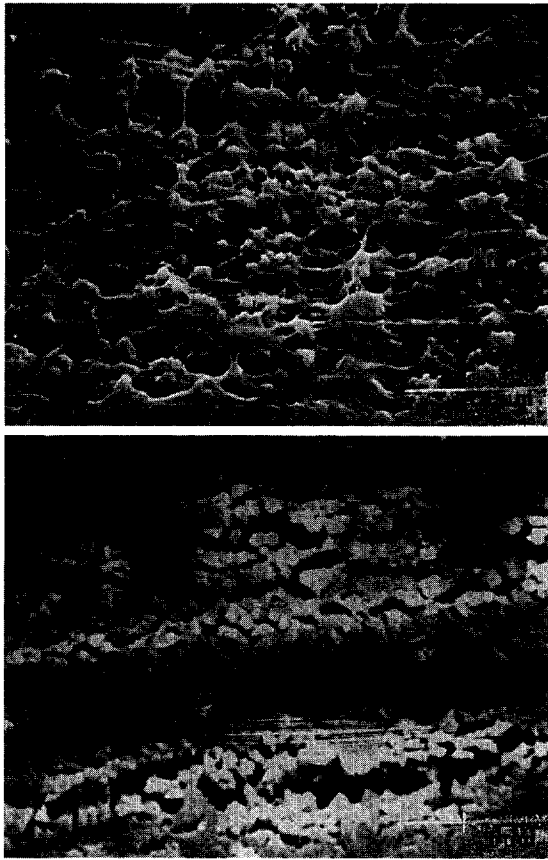


Fig. 5. Surface images of inside and outside of the hollow fiber membranes (top, outside; bottom, inside).

hol–water mixture (30 vol.% ethanol) to overcome the hydrophobicity of the PP membrane. Details of bubble point pressure measurement have been described elsewhere [17].

6. Effect of initial composition of melt solution

PP hollow fiber membranes were prepared according to the spinning conditions listed in the first row of Table 2. PP concentration was varied from 30 to 50 wt.%. The bubble point pressure increased nearly 10 times with increasing PP content from 30 to 50% as shown in Fig. 3, which means a decrease of the maximum pore size by a factor of 10. Cross sectional views of these membranes are presented in Fig. 4. Each sample has a lacy structure with interconnecting micropores as a result of spinodal decomposition accompanied by PP crystallization, since each sample has a smaller PP

composition than the monotectic composition and the bath temperature was cold enough to induce the thermodynamic conditions of both spinodal decomposition and PP crystallization based on the phase diagram (Fig. 1). Since the amount of diluent determines the porosity of the membrane, an increase of polymer content decreased the porosity. Pore size variation is shown in Fig. 4. However, the average pore size variation was not as much as that estimated by the bubble point pressure measurement. It is not clear how the bubble point variation was much greater than expected in the cross sectional images. Skin formation at the inner surface of the hollow fiber can be one of the possible causes.

The inner and the outer surfaces of the hollow fiber membrane were examined, the melt spinning conditions of which are listed in the second row of Table 2. As shown in Fig. 5, the membrane has an asymmetric structure and has a skin layer at the inner surface of the hollow fiber, though it is not as dense as those of the reverse osmosis membranes. The mechanism of skin layer formation was not clearly revealed. However, based on the mechanism of skin layer of a reverse osmosis membrane, it is probable that diluent vaporization at the surface forms the skin layer. The nitrogen gas was exposed to 458 K of the melt, therefore it should be heated up. Then the temperature of the inside of the hollow fiber melt was higher than that of the

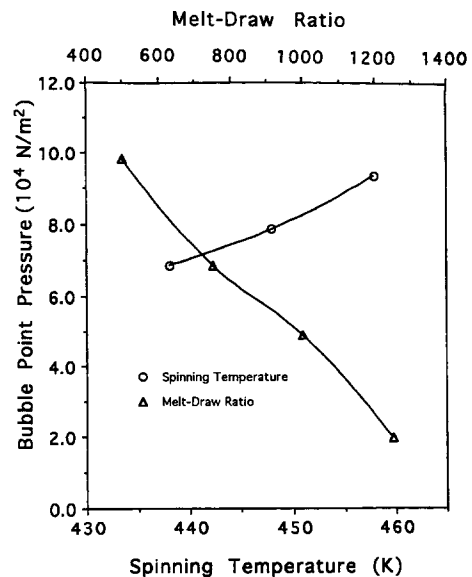


Fig. 6. Effects of spinning temperature and melt–draw ratio on the bubble point pressure of the hollow fiber membranes.

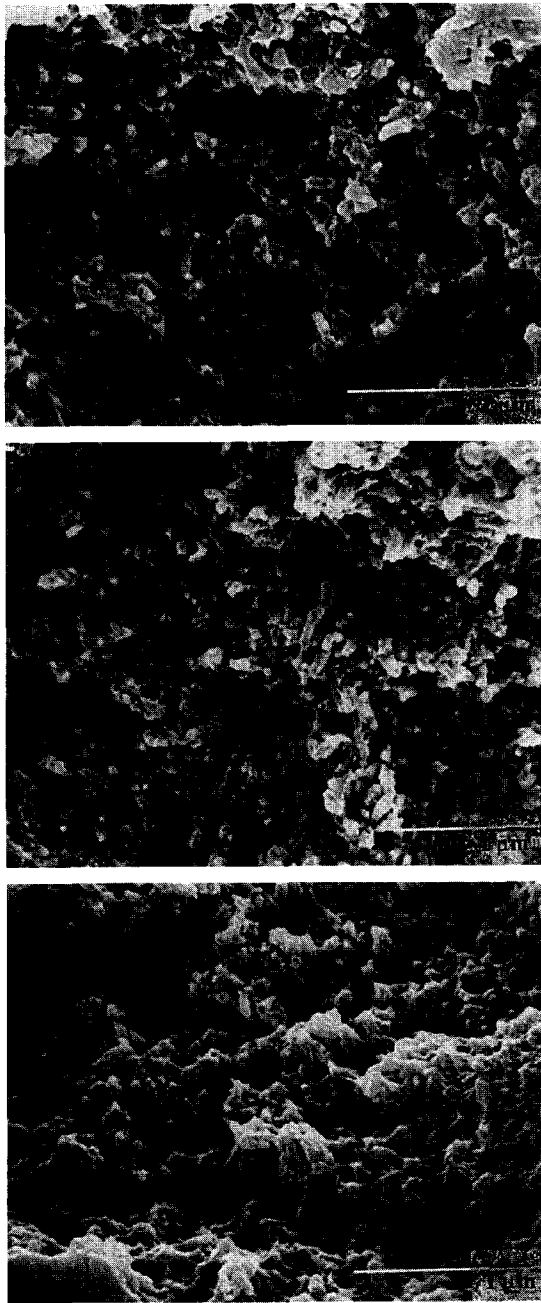


Fig. 7. Cross sectional images of the hollow fiber membranes spun at different temperatures (top, 438 K; middle, 448 K; bottom, 458 K).

outside, there might be diluent vaporization at the inside of the membrane, which resulted in a skin layer.

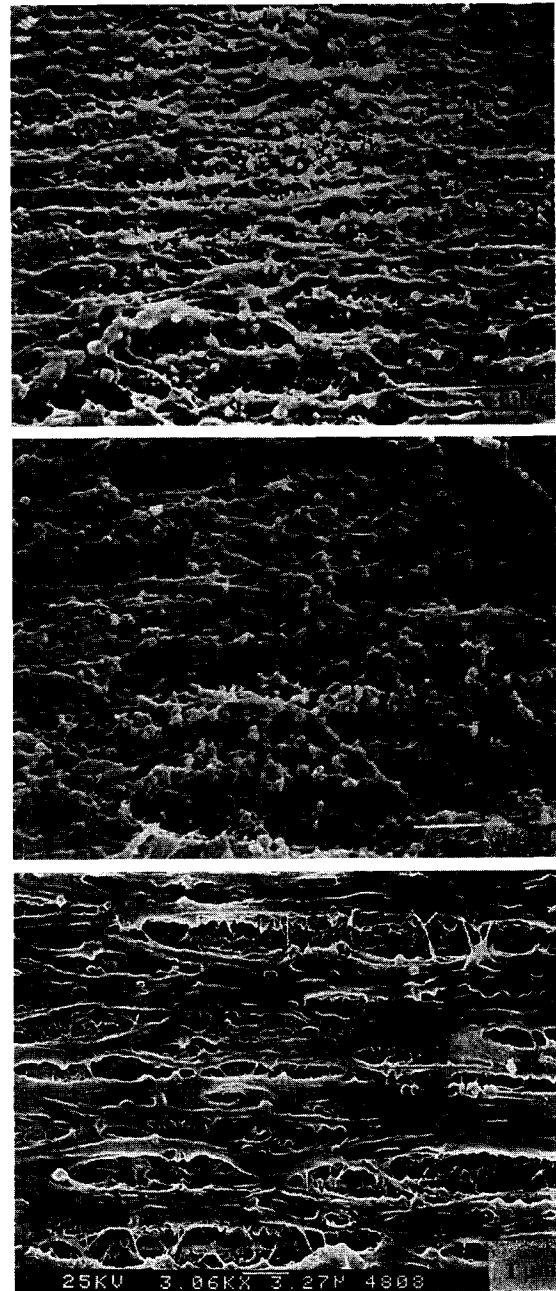


Fig. 8. Outer surface images of the hollow fiber membranes spun at different temperatures (top, 438 K; middle, 448 K; bottom, 458 K).

Skin layer formation gets more dense as the polymer content increases, which might reduce the maximum pore diameter at the inner surface, which caused the

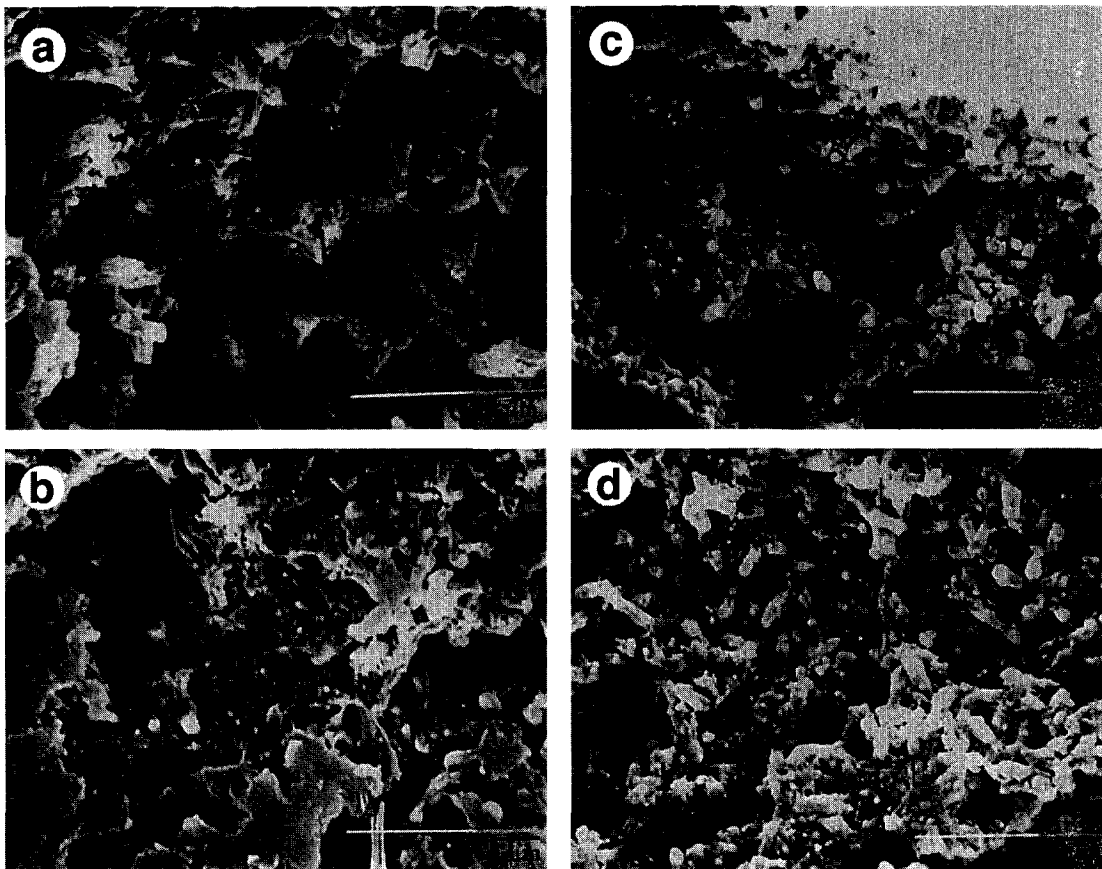


Fig. 9. Cross sectional images of the hollow fiber membranes prepared at different melt–draw ratios: (a) 500, (b) 750, (c) 1000 and (d) 1250.

remarkable bubble point pressure increase, which could not be expected from the cross sectional images in Fig. 4.

Since the initial PP composition was 40%, which is less than the monotectic composition, both surfaces underwent liquid–liquid phase separation followed by PP crystallization. The outer surface was exposed to cold quench medium, while the inner surface is exposed to nitrogen which is already heated by the surrounding polymer melt. Therefore, there should be significant temperature gradient difference between the two surfaces, which resulted in the different thermal histories and different phase separation rates. The temperature gradient difference played an important role in forming the structure of each surface via TIPS.

7. Effect of spinning temperature

Spinning temperature varied from 438 to 458 K with the other spinning conditions listed in the third row of

Table 2. Below a spinning temperature of 438 K, the hollow fiber solidified and melt-drawing was not uniformly performed. Above 458 K the spun fiber melt could not maintain its hollow form and collapsed due to the low viscosity of the melt. As shown in Fig. 6, the bubble point pressure slightly increased with increasing spinning temperature.

Since the viscosity of polymer melt solution increased by decreasing temperature, the stress on the polymer melt solution increased while it passed through the spinneret resulting in the increase of the degree of orientation of the hollow fiber. Therefore, the hollow fibers spun at lower temperature have a more oriented structure than those spun at higher temperature. A more oriented structure can have greater maximum pore size than the less oriented one [17]. However, the effect of spinning temperature is not as significant as the other factors. The cross sectional views of the membranes prepared at different spinning

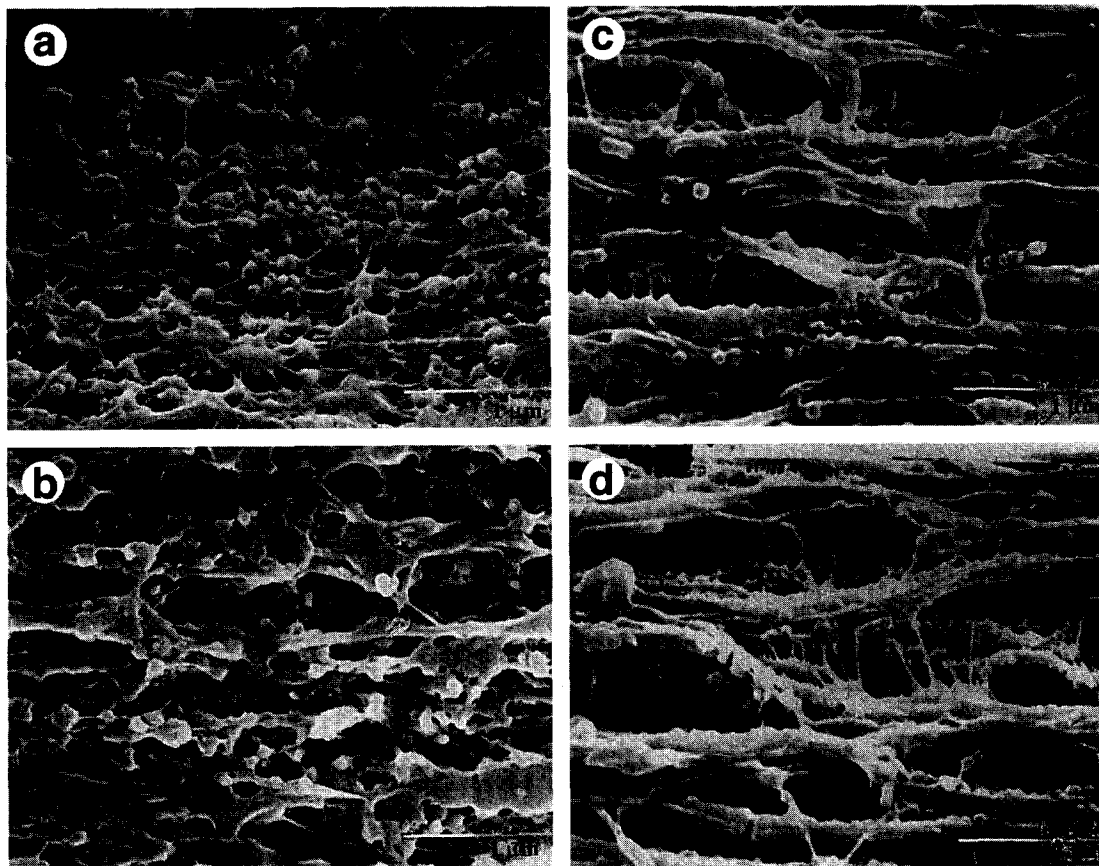


Fig. 10. Outer surface images of the hollow fiber membranes prepared at different melt-draw ratios: (a) 500, (b) 750, (c) 1000 and (d) 1250.

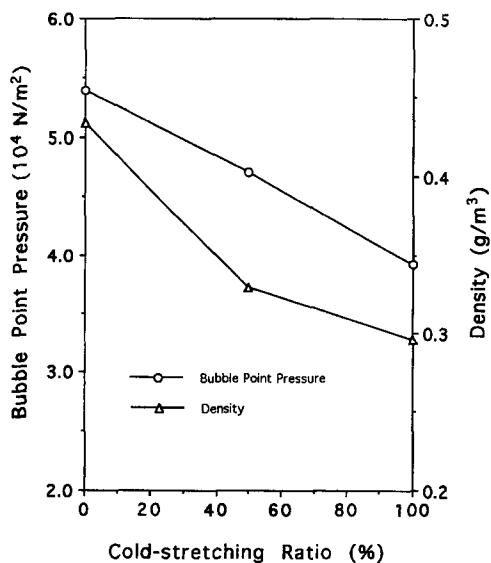


Fig. 11. Effects of cold-stretching on the bubble point pressure and the density of the hollow fiber membranes.

temperatures are shown in Fig. 7, in which pore size variation was not observed. Tiny PP spherulites were found in every sample indicating the liquid–liquid TIPS was followed by the solid–liquid TIPS.

There are structure differences at the outer surface of the membranes as shown in Fig. 8. The outer surfaces of the samples spun at 438 and 448 K have microporous structures not much different from the bulk structures. The sample spun at 458 K has a different surface structure from the bulk structure. A dense layer was formed at the surface on the same bulk structure. The mechanism of the dense layer formation might be similar to that of the skin layer at the inner surface. The fiber melt spun at higher temperature had greater vapor pressure of diluent than the lower temperature ones. Therefore, the dense layer was also formed in this case due to the greater vaporization of diluent. Though the dense layer formation mechanism was not clearly confirmed, the presence of this layer helps increase the

resistance, as illustrated by the bubble point pressure increase.

8. Effect of melt–draw ratio

The melt–draw ratio, defined as the ratio of take-up speed to the extrusion rate, was varied from 500 to 1250 with the other spinning conditions listed in the fourth row of Table 2. As the melt–draw ratio increased, the hollow fiber became more stretched and was thus more porous and more oriented to decrease the bubble point pressure as shown in Fig. 6. The cross sections of the membranes prepared at different melt–draw ratios are shown in Fig. 9. Outer surface structures of the membranes with different melt–draw ratios are shown in Fig. 10.

As expected, the fiber became more oriented in the spinning direction with increased melt–draw ratio especially in the outer surface images. For the highly melt–drawn samples (draw ratio of 1000 and 1250), a dense layer was formed at the outer surface due to directly contacting the coagulant before the fiber melt underwent liquid–liquid phase separation. The strand of the dense layer was aligned in the spinning direction, and the porous structure with tiny fibrils connecting each strand were developed due to cleavage. Since the porous structure was obtained via cleavage of the dense layer, tiny fibrils were formed in the direction perpendicular to the spinning direction.

9. Effect of cold-stretching

The hollow fiber membranes were prepared with the spinning conditions listed in the fifth row of Table 2. As mentioned in [8] and [17], micropores are formed via lamellae spreading via MSCS process of pure PP. Since microcrystalline lamellae are likely to align despite the presence of diluent in the TIPS process, a combination of TIPS and MSCS processes was attempted to make highly porous hollow fiber membranes. Microporous membranes made via TIPS were cold-stretched at 295 K and at a relative humidity of 52% at ratios of 50 and 100%, then they were annealed at 150°C for 1 min for relaxation.

As shown in Fig. 11, the bubble point pressure decreased with increase of cold-stretching ratio. Tiny

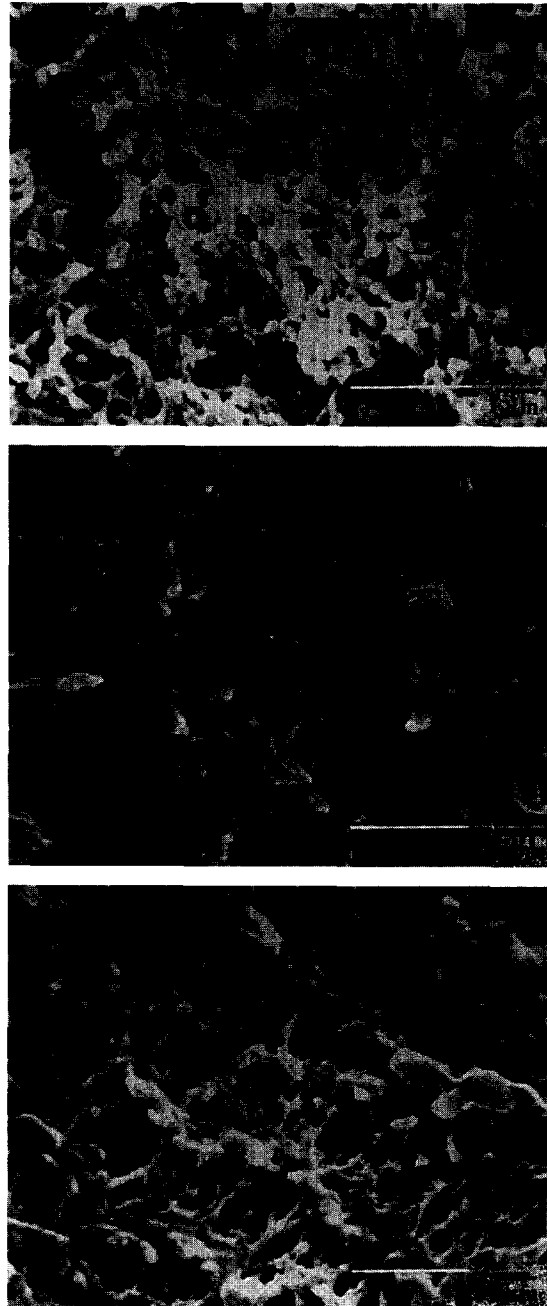


Fig. 12. Cross sectional image changes by cold-stretching (top, before cold-stretching; middle, 50% cold-stretched; bottom, 100% cold-stretched).

fibrils were developed via cold-stretching in its cross sectional views (Fig. 12). In this case the tiny fibrils were formed in the direction perpendicular to the spinning direction via cleavage as mentioned in effect of

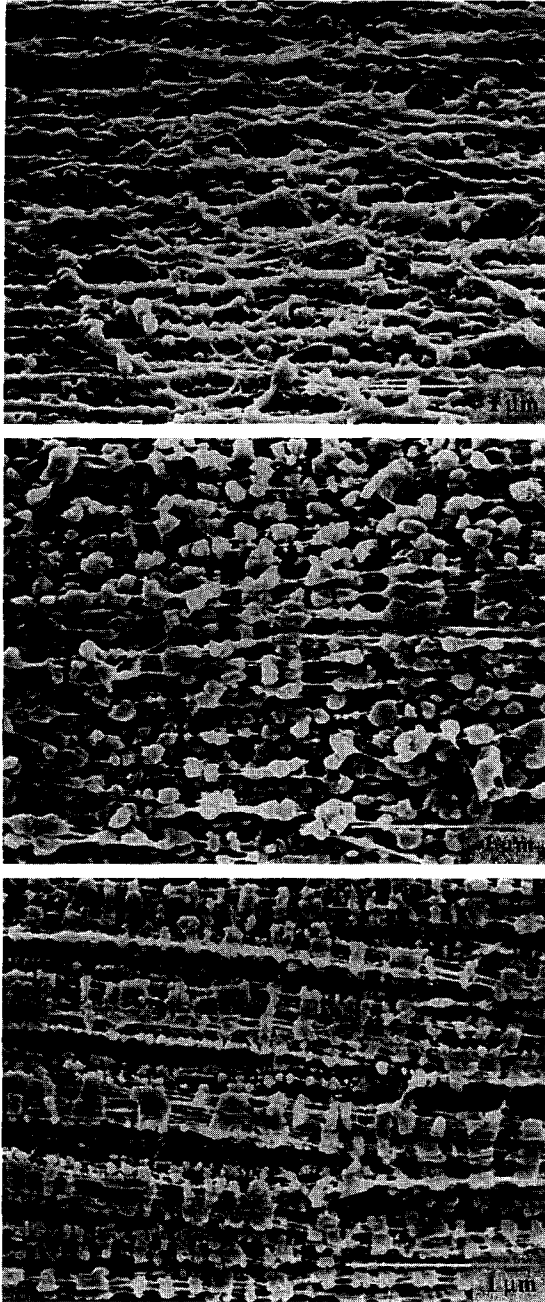


Fig. 13. Outer surface image changes by cold-stretching (top, before cold-stretching; middle, 50% cold-stretched; bottom, 100% cold-stretched).

melt-draw ratio section. Increases of porosity via cold-stretching were clearly observed in the cross sectional views. Cold-drawing enhanced the orientation of the hollow fiber membrane as observed at its outer

surface (Fig. 13). Stretching at the amorphous regions between the lamellae was observed, and the tiny fibrils along the spinning direction were also clearly seen in the 100% cold-stretched sample.

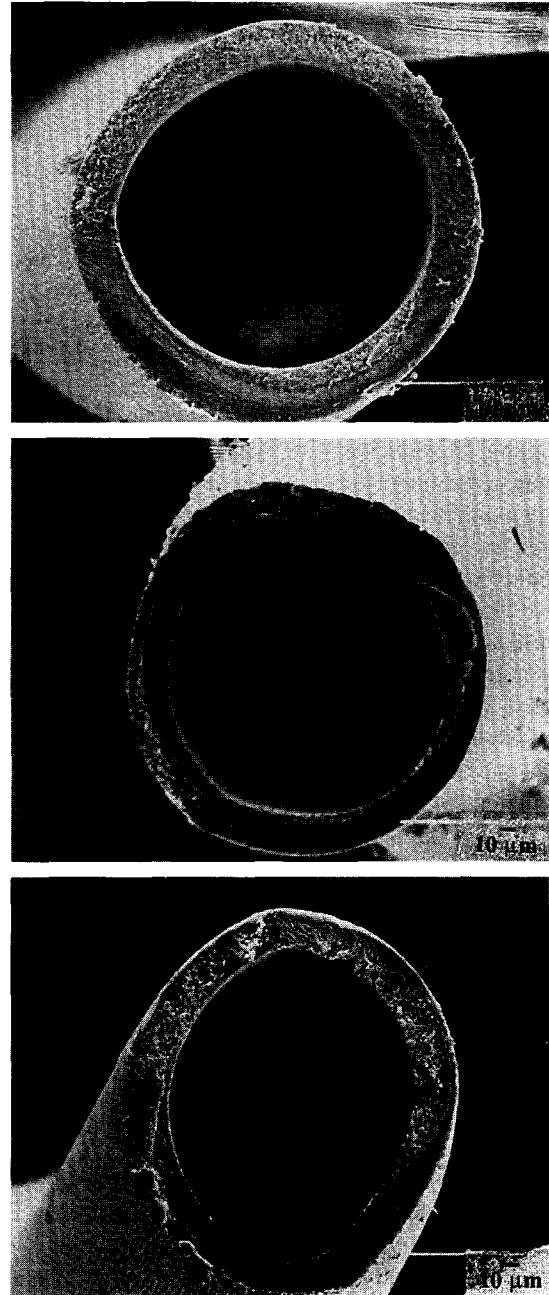


Fig. 14. Overview of the cold-stretched hollow fiber membranes (top, before cold-stretching; middle, 50% cold-stretched; bottom, 100% cold-stretched).

The fiber became thinner by increasing the melt-draw ratio. However, it is very interesting that the inner and outer diameters of the hollow fiber membrane were seldom changed after cold-stretching as shown in Fig. 14. Little change in dimension means the increase of volume to mass ratio of hollow fiber by cold-stretching, i.e. membrane porosity increase maintaining the original dimension. The density of each hollow fiber membrane was measured at 296 K using a density gradient column filled with an ethanol and water mixture according to ASTM D151-85 specification [17]. Density decreased as the cold-stretching ratio increased as shown in Fig. 11, which supports the porosity increase. However, the density decrease was less than that estimated from the mass balance. This is due to the incomplete wetting of the inside of the microporous membranes by the medium in the density gradient column.

The decrease of bubble point pressure produced by cold-stretching was not as significant as that via melt-drawing. While the bubble point pressure decreased from 9.8×10^4 to 4.9×10^4 N/m² by increasing 100% of melt-draw ratio from 500 to 1000 (Fig. 6), the bubble point pressure decreased from 5.4×10^4 to 3.9×10^4 N/m² by increasing 100% of cold-stretching ratio (Fig. 11). Since the volume of the hollow fiber doubled after 100% cold-stretching, the porosity increased by 100% from a rough estimation. But it does not mean doubling the maximum pore size.

10. Conclusions

The increase of PP composition in the initial melt solution decreased the porosity resulting in the increase of the bubble point pressure. The outer surface of the hollow fiber membrane was more porous than the inner surface due to the differences in the cooling rate and the initial diluent extraction rate in the coagulation bath. The spinning temperature effect was not as significant as the other parameters. Hollow fiber spun at lower temperature had greater melt viscosity resulting in a more oriented structure and smaller bubble point pressure than those spun at higher temperatures. The hollow fiber became more oriented by increasing the melt-draw ratio to enhance the formation of the micropores and fibril structure. Subsequent cold-stretching of the hollow fiber membranes prepared via TIPS remarkably

increased the membrane porosity, without any significant changes in the fiber dimensions. Tiny fibrils were formed both in the directions parallel and perpendicular to the spinning direction due to the stretching in the spinning direction and the cleavage of the hollow fiber.

References

- [1] J.J. Kim, J.R. Hwang, U.Y. Kim and S.S.Y. Kim, Membrane formation via thermally-induced phase separation from polypropylene/fatty acids systems, *Membrane (Japan)*, 19 (1994) 242.
- [2] G.H. Shipman, Microporous sheet materials, method of making and articles made therewith, US Pat., 4,539,256 (1985).
- [3] D.R. Lloyd, J.W. Barlow and K.E. Kinzer, Microporous membrane formation via thermally-induced phase separation, in K.K. Sirkar and D.R. Lloyd (Eds.), *New Membrane Materials and Processes for Separation*, AIChE Symp. Ser., No. 261, American Institute of Chemical Engineers, New York, NY, 1988.
- [4] S.S. Kim and D.R. Lloyd, Microporous membrane formation via thermally-induced phase separation. III. Effect of thermodynamic interactions on the structure of isotactic polypropylene membranes, *J. Membrane Sci.*, 64 (1991) 13.
- [5] S.S. Kim and D.R. Lloyd, Thermodynamics of polymer-diluent systems for thermally-induced phase separation. I. Determination of equation of state parameters, *Polymer*, 33 (1992) 1026.
- [6] S.S. Kim and D.R. Lloyd, Thermodynamics of polymer-diluent systems for thermally-induced phase separation. II. Solid-liquid phase separation systems, *Polymer*, 33 (1992) 1036.
- [7] S.S. Kim and D.R. Lloyd, Thermodynamics of polymer-diluent systems for thermally-induced phase separation. III. Liquid-liquid phase separation systems, *Polymer*, 33 (1992) 1047.
- [8] H.S. Bierenbaum, R.B. Isaacson, M.L. Druin and S.G. Plovan, Microporous polymeric films, *Ind. Eng. Chem. Prod. Res. Develop.*, 13(1) (1974) 2.
- [9] M.L. Druin, J.T. Loft and S.G. Plovan, Novel open-celled microporous film, US Pat., 3,801,404 (1974).
- [10] W.L. Gore, Process for producing porous products, US Pat., 3,953,566 (1976).
- [11] W.L. Gore, Very highly stretched polytetrafluoroethylene and process therefor, US Pat., 3,953,566 (1976).
- [12] K. Kamada, S. Minami and K. Toshida, Porous polypropylene hollow filaments and the method making the same, US Pat., 4,055,696 (1977).
- [13] M. Shino, T. Yamamoto, O. Fukunage and H. Yamamori, Process for making microporous polyethylene hollow fibers, US Pat., 4,530,809 (1985).
- [14] T. Tagawa, Piled-lamellae structure in polyethylene films and its deformation, *J. Polym. Sci., Polym. Phys. Ed.*, 18 (1980) 971.

- [15] S.S. Kim, G.B.A. Lim, A.A. Alwattari, Y.F. Wang and D.R. Lloyd, Microporous membrane formation via thermally-induced phase separation. V. Effect of diluent mobility and crystallization on the structure of isotactic polypropylene membranes, *J. Membrane Sci.*, 64 (1991) 41.
- [16] D.R. Lloyd, S.S. Kim and K.E. Kinzer, Microporous membrane formation via thermally-induced phase separation. II. Liquid-liquid phase separation, *J. Membrane Sci.*, 64 (1991) 1.
- [17] J.J. Kim, T.S. Jang, Y.D. Kwon, S.S. Kim and U.Y. Kim, Structural study of microporous polypropylene hollow fiber membranes made via melt spinning and cold-stretching method, *J. Membrane Sci.*, 93 (1994) 209.